Available online at www.sciencedirect.com

SCIENCE DIRECT®

Materials Chemistry and Physics 96 (2006) 9–15

MATERIALS CHEMISTRY AND PHYSICS

www.elsevier.com/locate/matchemphys

Effect of aging hardening on in situ synthesis magnesium matrix composites

Zhang Xiuqing *, Liao Lihua, Ma Naiheng, Wang Haowei

The State Key Laboratory of Metal Materials Composites, Shanghai Jiao Tong University, Shanghai 200030, China

Received 22 May 2005; received in revised form 30 May 2005; accepted 12 June 2005

Abstract

Magnesium matrix composites reinforced with TiC particulates was synthesized using in situ synthesis technique. The result of XRD revealed the presence of TiC in precursor blocks and TiC/AZ91 composites. Effect of aging hardening on the composites was described using Brinell hardness measurements and scanning electron microscopy (SEM). The results revealed that the aging hardening peak of TiC/AZ91 composite appeared earlier comparatively with that of AZ91 magnesium alloy. And the appearance of aging hardening peak was earlier under the higher aging temperature such as 200 °C. The precipitating behavior of $Mg_{17}Al_{12}$ phase in AZ91 alloy and TiC/AZ91 composites was described. Little discontinuous was discovered in the composites, and the amount of continuous precipitate in the composite matrix is smaller comparatively to that of AZ91 alloy. These results were analyzed with the fine grain size, much more interface between TiC and magnesium and high-density dislocation in magnesium matrix, which was contributed to the addition of TiC particulates.

Keywords: Magnesium matrix composite; In situ synthesis technique; Aging hardness; Microstructure characterization

1. Introduction

The ability of magnesium matrix composites to exhibit high-specific mechanical properties has been instrumental in attracting the attention of manufacturers for their possible use in automobile, aerospace, space, electronics and sports industries [1–3]. The heat-treated on materials can improve mechanical properties of materials, and retain the stability of materials structure and size. So some researches have been conducted on aging behavior of magnesium matrix composites. Badini et al. [4] investigated the aging characteristics of B_4C/AZ80 composite by optical microscopy and XRD. The addition of B_4C particle increased the aging rate of the composite. Zheng et al. [5] investigated the aging characteristics of SiC_w/AZ91 composite using differential scanning calorimetry (DSC), Vickers hardness measurement, scanning electron microscopy (SEM) and transmission electron microscopy (TEM). His results exhibited an accelerated hardening response compared with the unreinforced matrix alloy. Kiehn et al. [6] studied the electrical resistivity changes due to precipitation during isochronal annealing up to 300 °C in alumina fiber-reinforced AZ91D composite fabricated by squeeze casting. In a word, these researches indicate that the aging kinetics and aging hardening efficiency during aging of these composites depend on variety of factors, such as: the size; volume fraction of reinforcement; secondary processing; temperature of aging and the nature of matrix–reinforcement interface. But these results were all conducted on magnesium matrix composites which were synthesized using extra addition methods.

Compared to extra addition methods, in situ synthesis technique is a new processing method. The in situ synthesis technique is attractive on present research, for the composites synthesized by in situ method have advanced performance due to fine reinforcements and clear interface between metal matrix and reinforcement [7–9]. Remelting and dilution (RD) technique is one of in situ synthesis technique. The RD technique contains of two steps: firstly, precursor blocks contains of reinforcements is prepared; secondly, the precursor blocks is diluted into metal matrix materials melt to synthesize composites.

* Corresponding author. Tel.: +86 21 62932569; fax: +86 21 62932004.
E-mail address: wendya_zh@hotmail.com (Z. Xiuqing).

0254-0584/$ – see front matter
doi:10.1016/j.matchemphys.2005.06.027

Accordingly, the TiC/AZ91 composites were synthesized using RD technique. And particular emphasis was placed to study the formation of TiC/AZ91 composites and the effect of aging hardening on microstructure and Brinell hardness of TiC/AZ91 material.

2. Experimental procedures

The composite based on 8.0 wt.% TiC/AZ91 was prepared using the process of RD technique. The process was accomplished with three steps: (1) activated powder was synthesized by ball mill; (2) activated powder was sintered; (3) the precursor blocks were diluted into magnesium matrix melt to synthesize TiC/AZ91 composites.

In the experiment, the powder of Al, Ti and graphite whose purity degree are up 99.5% and the size are less than 75 μm were used as the base materials of precursor blocks. The powder mixture containing Al, Ti and graphite was milled and treated at argon gas atmosphere protection in order to activate the powder mixture. Then the mixed powder was pressed into columniform block with 30 mm diameter and 50 mm high. After being pressed, the precursor blocks were sintered in argon gas atmosphere protection.

The pure magnesium ingot was used as the base materials. After the magnesium ingot has been molten, the precursor blocks were diluted into the molten metal. The mixture melt was stirred to facilitate the incorporation and uniform distribution of reinforcement particulates in the metallic melt. Finally, the molten metal was poured into an iron sample mould to synthesize TiC/AZ91 composites. The AZ91 magnesium alloy was synthesized using common cast method. The matrix alloy and composite were solution-treated (T4). After solution treatment, the alloy and TiC/AZ91 composite were aged at 175 and 200 °C for different periods up to 50 h. The age-hardening response of the composite and AZ91 alloy was characterized using Brinell hardness measurements. Each hardness value is the average of at least five measurements. The microstructures of the AZ91 alloy and composite were examined by Hitachi S-520 scanning electron microscope (SEM).

3. Experimental results

3.1. Phase analysis

The XRD results of precursor blocks and TiC/AZ91 composites are shown in Fig. 1. The presence of TiC and Al_2O_3 phase in precursor blocks was validated. Aluminum as the base materials was also detected in precursor blocks using XRD analysis (as shown in Fig. 1(a)). Comparatively to precursor blocks, the presence of TiC phase and new $Mg_{17}Al_{12}$ phase in TiC/AZ91 composites was confirmed by XRD analysis, but Al_2O_3 and Al phase disappeared (as shown in Fig. 1(b)). The results of EDX analysis on TiC/AZ91 composites are shown in Fig. 2. The results of EDX analysis revealed that there are 6.43 wt.% titanium, 1.58 wt.% graphite and 8.36 wt.% aluminum in TiC/AZ91 composites. It can be calculated that there was about 8.01 wt.% TiC particulates in TiC/AZ91 composites for element titanium is being in composites by mean of TiC mainly. The weight percent of aluminum in TiC/AZ91 composites was consilient with that of AZ91 magnesium alloy.

3.2. Age-hardening response

The effect of aging time on the hardness of the TiC_p/AZ91 composite and the unreinforced AZ91 matrix alloy under

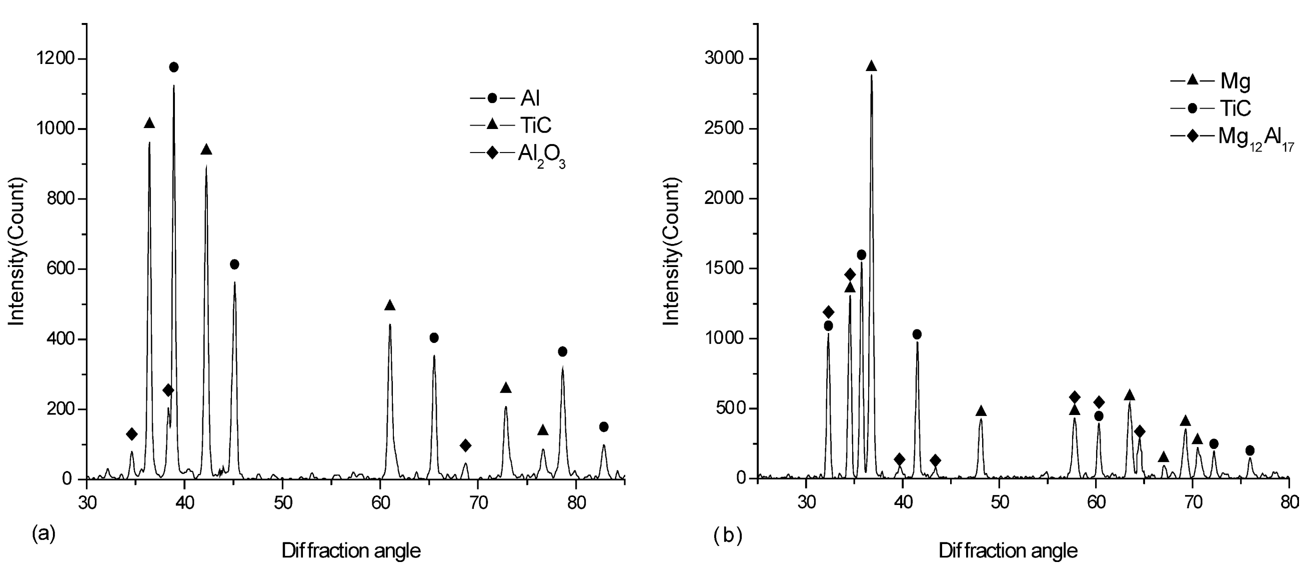

Fig. 1. XRD patterns of samples ((a) precursor blocks; (b) TiC/AZ91 composites).

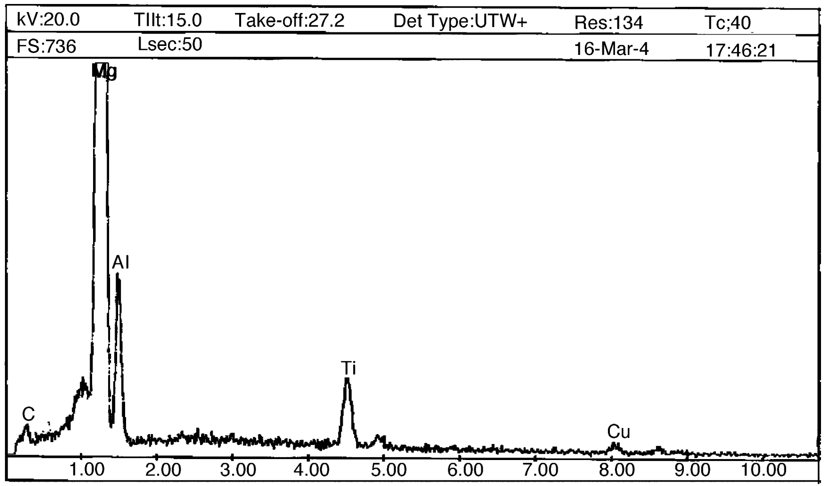

Fig. 2. EDX analyses of TiC/AZ91 composites.

175 and 200 °C is shown in Fig. 3. The hardness of the two materials increases monotonically as a function of aging time before reaching peak hardness. After reaching peak hardness, aging hardness of two materials is not increasing as the aging time increase, even it has little decreasing. The composite reaches peak hardness in 30 h at 175 °C, while the AZ91 magnesium alloy requires 40 h. The composite reaches peak hardness firstly (as shown in Fig. 3(a)). The effect of aging temperature on the peak-aging time for the composite as well as AZ91 alloy is also shown in Fig. 3. The composite reaches peak hardness in 12 h at 200 °C, while it requires 30 h at 175 °C. Similarly, the AZ91 magnesium alloy reaches peak hardness in 16 h at 200 °C, while it requires 40 h at 175 °C. The peak-aging time of materials at 200 °C is shorter than that of materials at 175 °C. At the same aging temperatures, the time to reach peak hardness is significantly less in the composite as compared with the monolithic alloy.

3.3. Microstructure observation

Figs. 4 and 5 show the SEM micrographs of AZ91 alloy and composites, which were aging-treated at 200 °C for different periods. After aging-treated for 2 h, discontinuous precipitates preferentially form at the grain boundaries in AZ91 alloy (as shown in Fig. 4(a)). Comparatively, discontinuous precipitates only form at the grain boundaries which zone has not TiC particulates in the composites, but continuous precipitates form mainly at the grain boundaries (as shown in Fig. 5(a)). With an increase of aging time, the discontinuous precipitation in AZ91 alloy ceases, and the continuous precipitates form in the remaining regions of the grain that are not occupied by discontinuous precipitates (as shown in

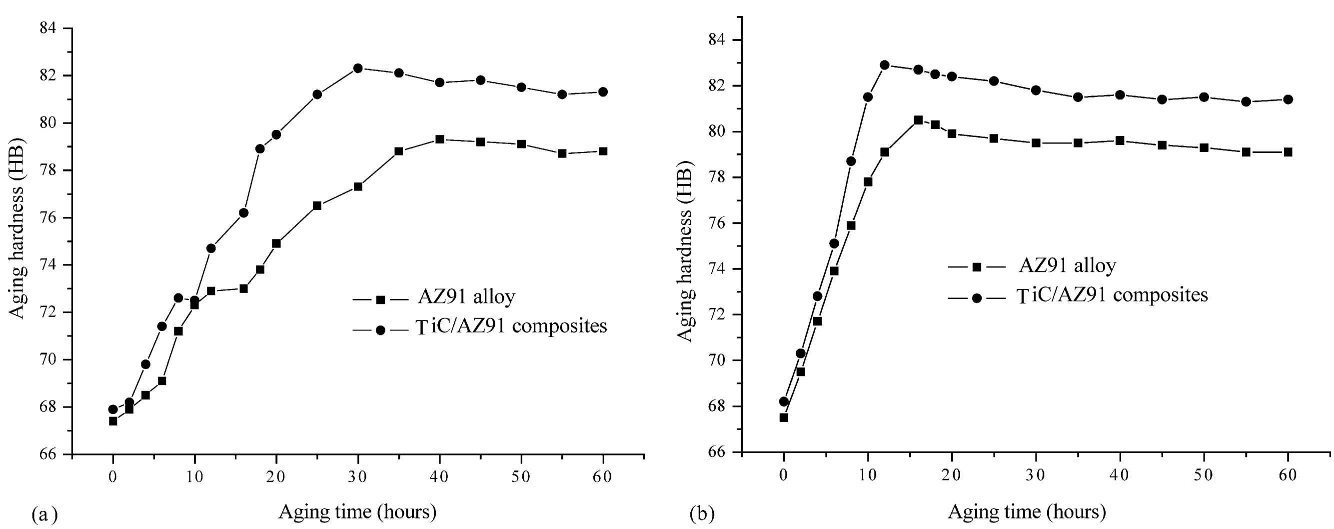

Fig. 3. The aging hardness corresponding to aging time at different aging temperature ((a) at 175 °C; (b) at 200 °C).

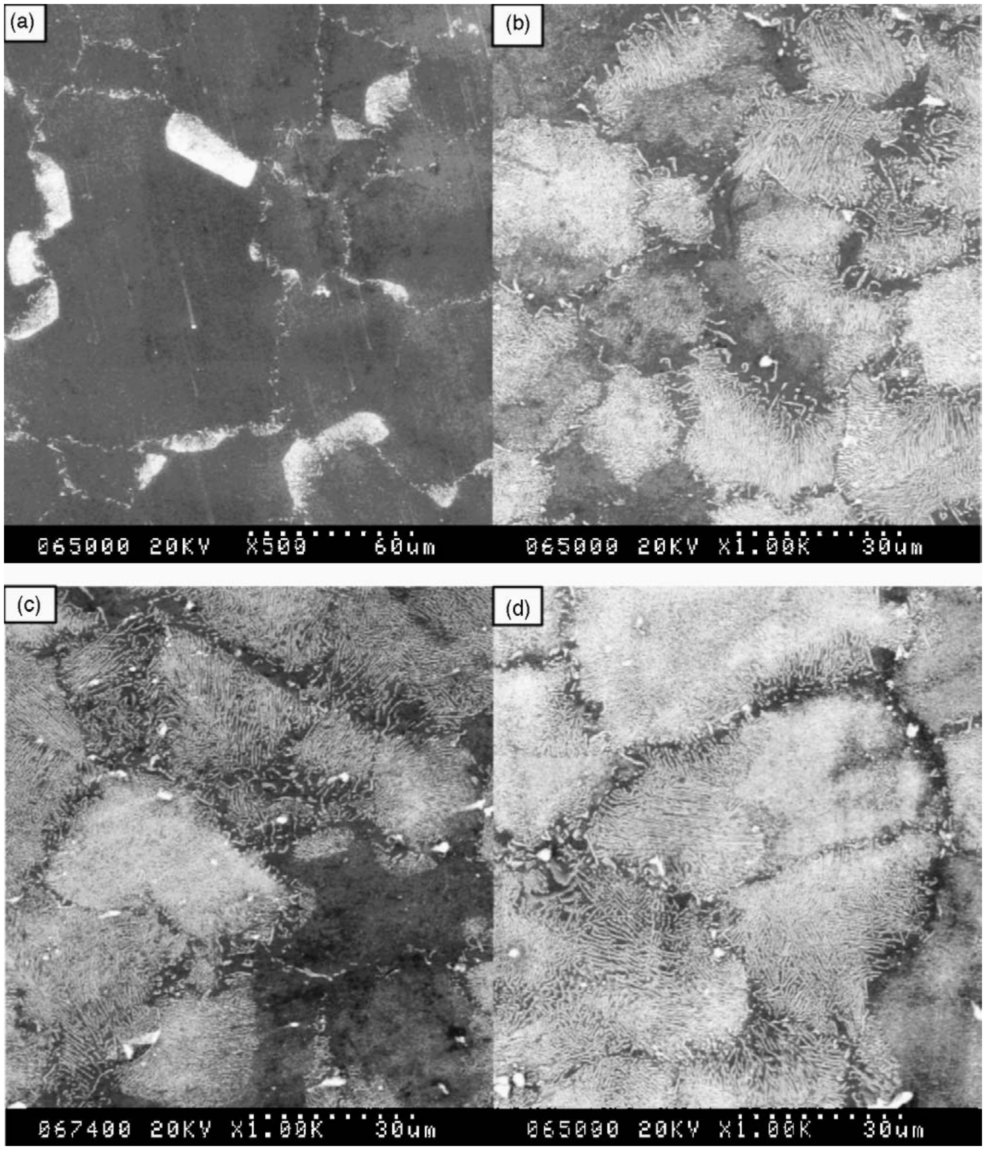

Fig. 4. SEM micrographs of AZ91 alloy at different aging time under 200 °C ((a) 2 h; (b) 8 h; (c) 12 h; (d) 16 h).

Fig. 4(b)). In the composites, the discontinuous precipitation ceases completely, and the distribution of continuous precipitates seems to be in homogeneous within AZ91 alloy. But in the TiC particulates-rich region, continuous precipitates are almost unobservable (as shown in Fig. 5(b)). At the peak-aging time, all of the grains contain cellular discontinuous precipitates at the grain boundaries and platelet continuous precipitates within the grains in AZ91 alloy (as shown in Fig. 4(c)). As same as in AZ91 alloy, the continuous precipitates in the composites spreads all over the grains except from TiC particulates zone. Additionally, the amount of continuous precipitate in the composite is smaller in comparison with that in AZ91 alloy (as shown in Fig. 4(c)). In the over-aged condition, both discontinuous and continuous precipitates became coarser in AZ91 alloy and the composites (as shown in Figs. 4 and 5(d)).

4. Discussion

During the sintering processing, the mixed powder as Al–Ti–C reacted. The reaction equation and its reacting free energy at 1400 K were listed as following [10]:

$$3\mathrm{Al} + \mathrm{Ti} \rightarrow \mathrm{TIAl_3} \quad Q = -3.724\,\mathrm{KJ\,mol^{-1}}$$

$$\mathrm{TiAl_3} + \mathrm{C} \rightarrow 3\mathrm{Al} + \mathrm{TiC} \quad Q = -74.02\,\mathrm{KJ\,mol^{-1}}$$

$$\mathrm{Ti} + \mathrm{C} \rightarrow \mathrm{TiC} \quad Q = -167.72\,\mathrm{KJ\,mol^{-1}}$$

It was presumable from those reaction equation that the mixed powders would react as the reaction equation: Al + Ti + C = Al + TiC ideally. So the final product of mixed powder after sintering process was TiC and aluminum ideally. The XRD results revealed the presence of TiC phase

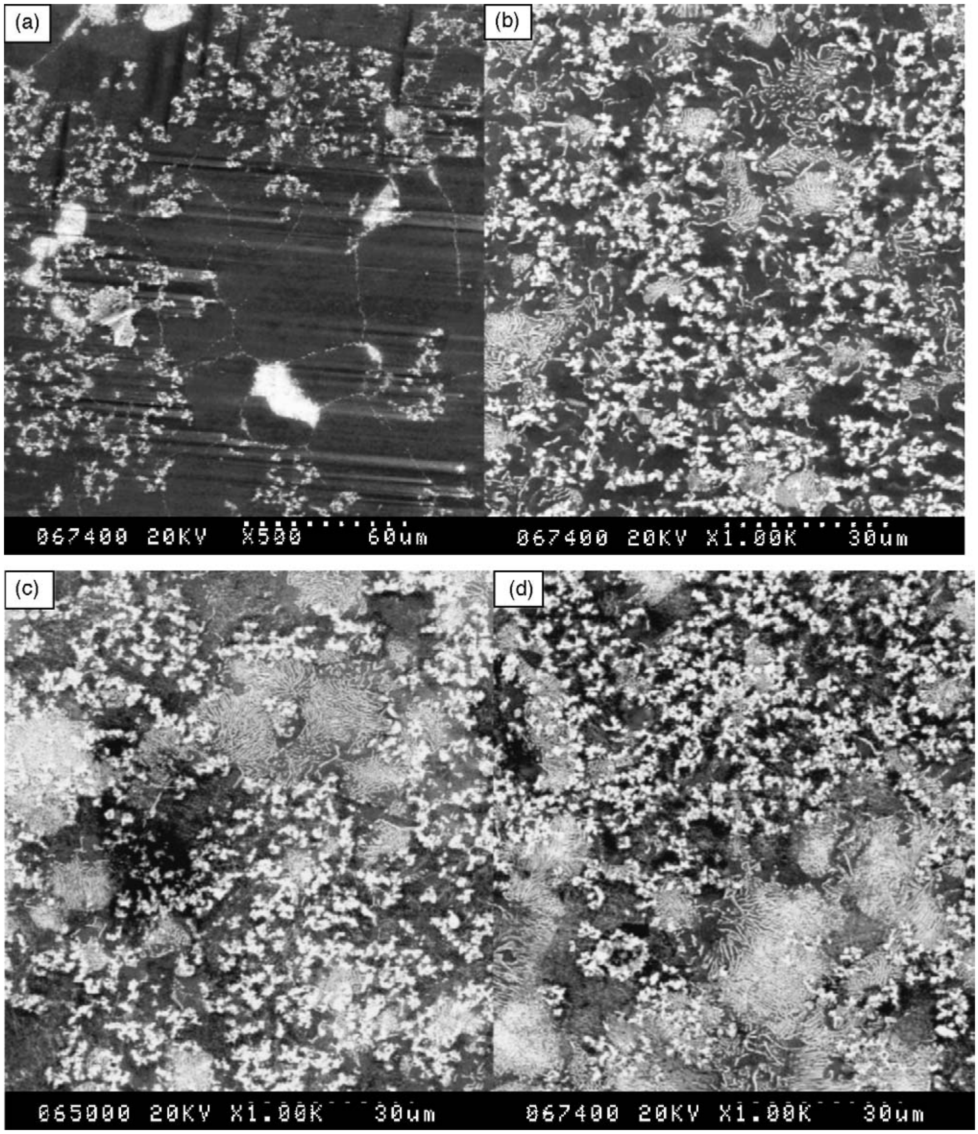

Fig. 5. SEM micrographs of TiC/AZ91 composites at different aging time under 200 °C ((a) 2 h; (b) 8 h; (c) 16 h; (d) 20 h).

in composites and precursor blocks sample for TiC is fine wettability to magnesium [11]. Al_2O_3 was discovered in the precursor blocks for aluminum was oxidized during mixing processing and sintering processing. Subsequently, the disappearance of Al_2O_3 in TiC/AZ91 composites is due to its poor wettability to magnesium. Aluminum in precursor blocks diffused into magnesium melts and formed $Mg_{17}Al_{12}$ phase reacting with magnesium during solidifying process. The presence of $Mg_{17}Al_{12}$ phase in the composites sample was identified, as showed in Fig. 3(b).

According to the age-hardening results, the TiC/AZ91 composite exhibits accelerated aging at two temperatures compared with the AZ91 alloy. In AZ91 alloy, the incoherent equilibrium phase $Mg_{17}Al_{12}$ precipitate without any interphase when it is in aging process. The generation type of $Mg_{17}Al_{12}$ phase is two as discontinuous precipitates and continuous precipitates. The discontinuous precipitates form firstly in the grain boundary and dislocation, and grow into transgranular in terms of laminated structure. Then the continuous precipitates form in transgranular after discontinuous precipitates cease. The continuous precipitates generate along with the base crystal plane (0 0 0 1) of magnesium matrix in term of fine-laminated structure, correspondingly, aluminum content in magnesium matrix decrease.

With the addition of TiC particulates, the grain size of TiC/AZ91 composites is smaller than that of AZ91 alloy, which ensure the more grain boundary in composites. Primarily, grain refinement results from nucleation of more new crystals from the melt, and subsequent growth of the new crystals to a limited size. More nucleation form in the magnesium melts because of addition of fine TiC particulates that become the host crystal. On the other hand, significant particle pushing effect is suggested by the appearance of many TiC particulates around the grains boundary. This phenomenon

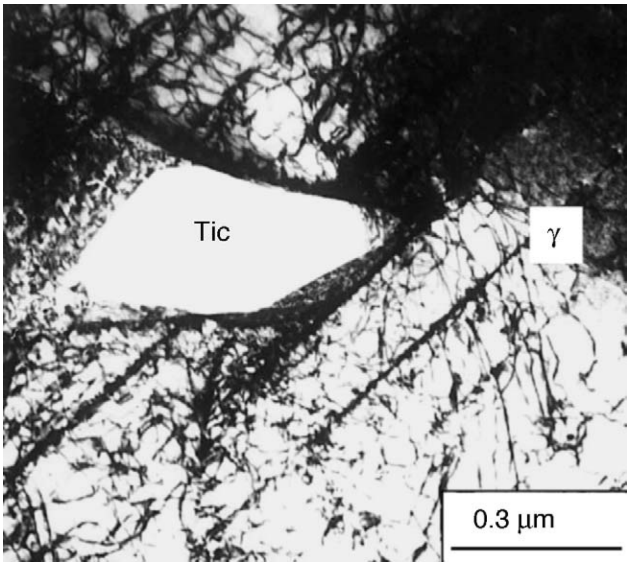

Fig. 6. Dislocation structures beside TiC particulates in TiC/AZ91 composites.

indicate that the growth rate of the primary phase may be reduced when the composites solidifies for TiC particulates present around the growing primary magnesium crystals could act as diffusion barriers to their growth. Consequently, the restricted growth of the primary phase would allow the melt to have sufficient time to create more nuclei. Therefore, a fine grain size of the TiC/AZ91 composites is achieved in the resulting solidified microstructure, which is validated by Fig. 5(a). The fine grain size of composites results in more grain boundary in magnesium matrix, which ensures the more nucleation of $Mg_{17}Al_{12}$ phase. For $Mg_{17}Al_{12}$ phase preferential nucleate in grain boundary. More interfaces between TiC and magnesium generate because of addition of TiC particulates. The interfaces provide efficient diffusion path of the Al element. The efficient diffusion path accelerates the precipitation of $Mg_{17}Al_{12}$ phase. Then the TiC/AZ91 composite exhibits accelerated aging compared with the AZ91 alloy. And aging hardness peak of composites is early compared with the AZ91 alloy.

The high-density dislocation in the composite is also an important factor to accelerate the precipitation. The high-density dislocations are introduced by the large differences in the coefficient of thermal expansion (CTE) between TiC particulates ($3.0 \times 10^{-6}\,K^{-1}$) and AZ91 alloy ($26.0 \times 10^{-6}\,K^{-1}$). This thermal mismatch will result in a substantial stress within the matrix around the TiC particulates during cooling from the solution-treated temperature. The residual stress can result in high-density dislocation in the vicinity of the TiC particulates (as shown in Fig. 6). Matrix dislocations is recognized as the preferential nucleation sites for $Mg_{17}Al_{12}$ precipitates for solution atoms will have enhanced diffusion rates along the dislocations via pipe diffusion [12–14]. The high-density dislocation within the matrix near the TiC particulates increases the rate of Al atom diffusion to particulates–matrix interface. Also the high-density dislocations serve as preferential nucleation sites of $Mg_{17}Al_{12}$, markedly increasing the rate of age-hardening of composites. So the high-density dislocation in magnesium matrix also accelerates the precipitation of $Mg_{17}Al_{12}$ phase.

In a word, the accelerated aging is attributed to the addition of TiC particulates in magnesium matrix which accelerate the precipitation of $Mg_{17}Al_{12}$ phase. The acceleration of the precipitation can be explained by the following possible mechanism: (1) much more grain boundary provides more preferential nucleation sites for precipitation; (2) much more interfaces between TiC and magnesium enhance effective diffusion path of aluminum in composite; (3) high-density dislocations in the composite enhance nucleation of the precipitates.

The aging temperature is a factor of high importance on aging hardening time. According to diffusion coefficient equation [15]: $D = D_0 \exp(-\frac{Q}{RT})$, the diffusion rate increases when aging temperature increases, where D and D_0 is the diffusion coefficient, Q is diffusion activation energy, T is diffusion temperature, and R is constant. So the precipitation is accelerated under high-aging temperature for the diffusion speed of Al element becomes fast. The appearance of aging hardening peak of composites prefers to high-aging temperature (as shown in Fig. 3).

5. Conclusions

Magnesium matrix composites reinforced with TiC particulates was synthesized using RD technique successfully. Compared with the AZ91 alloy, accelerated aging is discovered in the TiC/AZ91 composite. The addition of TiC particulates can bring on the fine grain size, more interface between TiC and magnesium and high-density dislocation in magnesium matrix, which accelerate the precipitates of $Mg_{17}Al_{12}$ phase. The aging temperature is also an important factor on aging hardening time. The appearance of aging hardening peak of composites and AZ91 alloy prefers to high-aging temperature such as 200 °C for the diffusion rate of Al element become fast on high-aging temperature.

Acknowledgment

The authors thank State Key Lab of Metal Materials Composites for providing the XRD, SEM and Brinell hardness testing.

References

[1] Y. Kojima, Mater. Sci. Forum 350–351 (2000) 3–18.
[2] E. Aghion, B. Bronfin, Mater. Sci. Forum 350–351 (2000) 19–28.
[3] A. Luo Alan, Mater. Sci. Forum 419–422 (2003) 57–66.
[4] C. Badini, F. Marino, M. Montorsi, X.B. Guo, Mater. Sci. Eng. A157 (1992) 53–61.

[5] M.Y. Zheng, K. Wu, S. Kamado, Y. Kojima, Mater. Sci. Eng. A 348 (2003) 67–75.
[6] J. Kiehn, K.U. Kainer, P. Vostry, I. Stulikova, Phys. Status Solidi A 161 (1997) 85–95.
[7] P.C. Maity, S.C. Panigrahi, Key Eng. Mater. 104–107 (1995) 313.
[8] S.C. Tjong, Z.Y. Ma, Mater. Sci. Eng. R 29 (2000) 49–113.
[9] K.L. Tee, L. Lu, M.O. Lai, Compos. Struct. 47 (1999) 589–593.
[10] D.L. Ye, Thermodynamics Date Handbook of Practical Inorganic Matter, Metallurgical Industry Press, Beijing, 1981.
[11] A. Contreras, et al., Scripta Mater. 48 (12) (2003) 1625–1630.
[12] A.F. Crawley, Acta Metall. 22 (1974) 557–562.
[13] A.F. Crawley, B. Lagowski, Metall. Trans. 5 (1974) 949–951.
[14] S. Celotto, Acta Mater. 48 (2000) 1775–1787.
[15] G.X. Hu, X. Cai, The Base of Materials Science, Shanghai Jiao Tong University Press, Shanghai, 2000, pp. 136–137.